

## Original Article

# Epitope-guided selection of CXCR4-targeting antibodies using AlphaFold3 for GPCR modulation and cancer therapy

Srimathi Venkataraman<sup>1\*</sup>, Yi-Chuan Li<sup>2\*</sup>, Zi-Wei Hung<sup>3</sup>, Yu-Chieh Hsu<sup>4</sup>, Zhuo Yang<sup>5</sup>, Tsung-I Tsai<sup>5</sup>, Mien-Chieh Hung<sup>3,4,6</sup>, Kyung Ho Han<sup>7</sup>, Chih-Wei Lin<sup>3,4,6</sup>

<sup>1</sup>Graduate Institute of Biological Science and Technology, China Medical University, Taichung 406040, Taiwan; <sup>2</sup>Department of Biological Science and Technology, China Medical University, Taichung 406040, Taiwan; <sup>3</sup>Institute of Biochemistry and Molecular Biology, China Medical University, Taichung 406040, Taiwan; <sup>4</sup>Graduate Institute of Biomedical Sciences, China Medical University, Taichung 406040, Taiwan; <sup>5</sup>Department of Chemistry, The Scripps Research Institute, La Jolla, California 92037, United States; <sup>6</sup>Cancer Biology and Precision Therapeutics Center, and Center for Molecular Medicine, China Medical University, Taichung 406040, Taiwan; <sup>7</sup>Department of Biological Sciences and Biotechnology, Hannam University, Daejeon 34054, Republic of Korea. \*Equal contributors.

Received March 4, 2025; Accepted April 21, 2025; Epub May 15, 2025; Published May 30, 2025

**Abstract:** G protein-coupled receptors (GPCRs) play important roles by transmitting signals when they bind to specific ligands in human. Dysregulation of the GPCRs has been associated to metabolic diseases, inflammatory and cancers, and making them key targets for therapeutic intervention. The structural characterization of GPCR-ligand interactions remains challenging due to the difficulty in obtaining complex structures. In this study, we chose CXCL12 chemokine receptor 4 (CXCR4), a member of the GPCR family, as the receptor and employed AlphaFold3 to predict the interaction sites between ligands and GPCRs. The results show that the extracellular loop 2 (ECL2) region is crucial for CXCL12-CXCR4 interactions. Using this epitope-guided approach, we selected antibodies from a combinatorial library that bind to CXCR4 and block CXCL12 signaling. Two antibodies, C5 and F4, were found to inhibit CXCL12 signaling in reporter cell lines. Furthermore, these antibodies also exhibited antibody-dependent cellular cytotoxicity against the acute T cell leukemia cell line and the B cell lymphoma cell line. This approach provides a promising way to develop effective antibodies for treating CXCR4-expressed cancer cells, as well as for other diseases linked to GPCR dysfunction.

**Keywords:** GPCR, CXCR4, CXCL12, antibody, phage display, AlphaFold3

## Introduction

G protein-coupled receptors (GPCRs) are one of a large family, consisting of more than 800 members, distributed in various organs and tissues of the human body, including the central immune system, and cardiovascular system. GPCRs exhibit a conserved structure characterized by an extracellular N-terminal segment, seven transmembrane regions, and a cytoplasmic C-terminal region. These receptors are capable of sensing a diverse array of ligands, including peptides, and proteins. Upon binding with these ligands, GPCRs undergo conformational changes that activate intracellular signaling pathways [1, 2]. The binding of an agonist to

a GPCR induces a conformational change, facilitating interaction with heterotrimeric G proteins. This activation prompts the exchange of guanosine diphosphate (GDP) for guanosine triphosphate (GTP) and the dissociation of G protein subunits. The G $\alpha$  and G $\beta\gamma$  subunits then activate downstream signaling pathways, altering intracellular levels of cyclic adenosine monophosphate (cAMP) or calcium and influencing physiological processes. This illustrates the vital role of GPCRs in cellular signaling [2-5]. Dysregulation of the GPCRs is associated with a number of metabolic diseases, autoimmune, inflammatory diseases and cancers, therefore the GPCR is often targeted for treatment of many diseases for drug targets [6-9]. The devel-

## Selection of GPCR targeting antibody via AlphaFold3

Development of effective and specific therapeutic agents targeting GPCRs poses a significant challenge. This challenge is primarily attributed to the inherent difficulty in purifying and crystallizing GPCRs, which is a consequence of their complex transmembrane structures [10, 11]. This difficulty and complexity limit the determination of their complete structures, which is crucial for drug design. Recent advances in artificial intelligence (AI)-driven protein structure prediction, such as AlphaFold3 (AF3) by DeepMind and approaches developed by David Baker's group, have revolutionized this field [12-16]. AF3 represents a major breakthrough in AI-driven structural biology, enabling precise predictions of multi-molecular interactions, including ligand-receptor binding sites. These AI methods significantly accelerate protein and antibody discovery by providing accurate structural insights.

Antibody therapy has become a major new drug class developed in recent years due to its high specificity and low adverse effects, and more than 100 antibodies have been approved and many are in clinical trials [17-21]. Most antibodies were isolated and developed from hybridoma and combinatorial antibody library [22]. The advantage of combinatorial antibody library leverages the immense diversity of binding molecules, thus allow researchers to facilitate basic studies and isolate clinical candidates with optimal binding and functional properties in vitro screening experiments. Antibodies selected from these libraries exhibit a range of mechanisms, functioning as neutralizers, agonists, or antagonists [23-27]. The combinatorial antibody library is still an important tool applied for biomedical applications.

CXC chemokine receptor 4 (CXCR4) is a GPCR that was first identified as a coreceptor for human immunodeficiency virus (HIV), and was later reported to be associated with leukocyte trafficking and cancers [28-31]. CXCR4 binds to its ligand CXCL12, also known as stromal cell-derived factor 1 (SDF-1) and mediates tumor growth and metastasis. Recent studies showed that CXCR4-CXCL12 axis also modulate the immune microenvironment in cancer e.g. pancreatic cancer and AML (Acute myeloid leukemia) and inhibition of the CXCR4-CXCL12 pathway enhanced T cell access to the tumor microenvironment. These insights suggest that tar-

geting the CXCR4-CXCL12 axis could be a transformative strategy for improving cancer immunotherapy and patient outcomes [32, 33]. In addition, CXCR4 mediates CD47 internalization and downstream antitumor in a mouse model of mesothelioma [34]. Taken together, these findings support that targeting the CXCR4-CXCL12 axis offers the possibility of affecting CXCR4-expressing cancer cells, modulating immune responses, or synergizing with other targeted anti-cancer therapies [33].

In this study, GPCRs and their ligands are critical therapeutic targets for numerous diseases. However, structural characterization of GPCR-ligand interactions remains challenging due to the difficulty in obtaining complex structures. We chose CXCR4 and employed AF3 to predict the interaction sites between ligands and further for antibody selection. This approach may provide a promising way to develop effective antibodies for treating CXCR4 expressed cancer cells and for applications in other diseases associated with GPCR dysfunction.

### Materials and methods

#### *Reagents and cell culture*

HEK293T cells were maintained in DMEM medium (Gibco #119650) with 10% FBS. The FreeStyle 293-F cells (Invitrogen) were cultured in FreeStyle293 Expression Medium (#K900001, Invitrogen). CXCR-4 overexpressed 293T cells were generated by lentivirus containing CXCR4 sequence (UniProt, P61073) and maintained in DMEM medium with 10% FBS. The Tango CXCR4-bla U2OS cell line (#K1779; Thermo Fisher Scientific) was maintained according to the manufacturer's instructions. The Jurkat and Romas cells were maintained in RPMI 1640 medium with 10% FBS.

#### *Model CXCR4-CXCL12 complex structure*

We utilized AlphaFold 3 server (<https://alphafoldserver.com/>) to predict the structure of the CXCR4-CXCL12 complex. We retrieved amino acid sequences of CXCR4 (P61073) and CXCL12 (P48061) from Uniprot databank. In order to obtain a high-confidence structural model and assess reproducibility, the template sequence was loaded as input in AlphaFold server for twenty times. The resulting models were evaluated based on the confidence met-

## Selection of GPCR targeting antibody via Alphafold3

rics as predicted Local Distance Difference Test (pLDDT), interface predicted Template Modelling score (ipTM), and predicted Template Modelling score (pTM), Root-Mean-Square Deviation (RMSD) consistency, and overall structural stability. The model with the highest confidence score and structural quality was chosen for further analysis. We further analyzed essential interactions of extracellular regions of the CXCR4 by using a distance cut off  $<4 \text{ \AA}$  from CXCL-12 in pyMOL. Further, we validated our predicted AF3 structure by aligning it with the Cryo-EM structure. To determine the structural similarity, RMSD and C $\alpha$  RMSD values for the superimposed structure were generated using pyMOL. To visualize and analyze the structural details, all graphical representations of the protein models were generated using PyMOL version 2.5.5 (Schrödinger, LLC).

The selection of CXCR4 antibody from combinatorial antibody library. The peptide consisting of ECL2 of CXCR4 (ANVSEADDRY ICDRFYPNDLW) with biotin labeled was synthesized (Genscript), and used for phage panning. The panning procedure followed a modified protocol as described previously [35]. Briefly, the amplify phage particles displaying a combinatorial scFv antibody library with  $10^{11}$  diversity were incubated with ECL2 antigen. Streptavidin coated magnetic beads (1:1000 dilution; #21925, Pierce) were then added to the solution to pull down the phage-bound biotinylated antigen. Bound phages were eluted with glycine-HCl (pH 2.7) after 3 washes with PBST (0.05% TWEEN20 in PBS pH 7.4). To remove unbound phages, and used in the following infection of XL-1 blue cells (#200228; Agilent). The infected cells were used for next round of panning in the presence of helper phage VCSM13 (Agilent #200251). After three to four rounds of enrichment, the colonies were picked and confirmed by phage ELISA. The positive clones were picked for DNA sequencing. The six independent sequences were confirmed. The VH and VL families were analyzed by the international ImMunoGeneTics information system (IMGT).

### ELISA

NetruAvidin (#31000; Thermo Scientific) was diluted in carbonate-bicarbonate buffer to a final concentration of 2  $\mu\text{g/ml}$  in 96-well ELISA

plates (Corning Costar) at 4°C overnight. The next day, the wells were washed with TBST buffer (0.05% TWEEN20 in TBS pH 7.4). All peptides are synthesized with biotin at the C-termination. N-terminal peptide (MEGISIYTS-DNYTEEMGSGDYDSMKEPCFR EENANFNK), ECL1 peptide (ANWYFGNFLCK), ECL2 peptide (ANVSEADDRY ICDRFYPNDLW), ECL3 peptide (DSFILLEIIKQGCEFENTVHK). Add 100 ng of N-terminal peptide, ECL1, ECL2 and ECL3 per well in TBS at pH 7.4, incubate for 1 hour, and then block with 5% milk at 37°C for 1 hour. After the washing step, add 50  $\mu\text{L}$  of phage samples or purified antibody to each well, incubate for 1 hour, and then wash. Anti-M13 HRP conjugated secondary antibody (1:5,000 dilution; #11973-MM05T-H, Sino) or anti-human Fc HRP conjugated secondary antibody (1:10,000 dilution; #A80-104, Bethyl) was added to the wells, incubated for 1 hour, and then washed 5 times with TBST, and then 50  $\mu\text{L}$  of TMB solution (T4444, Sigma) was added to each well. Then add 50  $\mu\text{L}$  of TMB solution (#116843-02001; Roche). Absorbance was measured at 405 nm on a plate reader (PerkinElmer).

### Expression of CXCR4 antibodies

The candidate scFv antibodies were cloned into a pFuse expression vector (#pfuse-hg1; InvivoGen) for expression of scFv-Fc proteins with the entire Fc domain of human IgG1. For antibodies in the full-length IgG1 format, variable regions of heavy chain and light chain (VH and VL) from the scFv sequence were cloned into plasmids with the complete constant domains of IgG1 heavy chain and light chains. The FreeStyle 293-F cells were transfected with the scFv-Fc expression plasmid or co-transfected with equimolar heavy and light chain plasmids and cultured for 5 days. Antibodies in the culture medium were purified by HiTrap Protein A HP column (#17-0403-03; GE Healthcare) from ÄKTA express purifier (GE Healthcare) and protein concentration was determined using a nanodrop spectrophotometer.

### Flow cytometry

The 293T-CXCR4 stable cell line was generated by lentivirus, and 293T cells ( $5 \times 10^5$ ) were stained with 1  $\mu\text{g}$  of dissociated CXCR4 antibody in 100  $\mu\text{L}$  of FACS buffer (PBS with 1% FBS), incubated for 30 min in an ice bath for 30

## Selection of GPCR targeting antibody via AlphaFold3

min, and the cells were washed twice with FACS buffer and incubated for 30 min at 4°C with secondary antibody Alexa Fluor™ 488 goat anti-human IgG (H + L) (1:1000; #A11013, Invitrogen) for 30 min. After washes with FACS buffer, the cells were analyzed by using CytoFLEX S (Beckman Coulter).

### *Cell cytotoxicity assay*

The PBMCs were collected from blood samples of healthy donors, the cancer cells were incubated with CXCR-4 antibodies and PBMC. The cytotoxicity was measured by lactate dehydrogenase (LDH) release using CytoTox 96® Non-Radioactive Cytotoxicity Assay (Promega, G1780). and LDH release was measured according to the manufacturer's instructions.

### *Tango CXCR4-bla reporter assay*

The Tango CXCR4-bla U2OS cells contain the human CXCR4 linked to a TEV protease site and a Gal4-VP16 transcription. Once ligands bind to hCXCR4 and trigger desensitization of membrane, the intracellular arrestin-protease fusion protein is recruited to the activated receptor gene. In this reporter cells Tango™ CXCR4-bla U2OS (#K1779, Thermo). Briefly, Tango CXCR4-bla U2OS cells were plated at around 20,000 cells per well for overnight. The CXCL12 were mixed with to measure their agonist effects. For inhibition studies of CXCR4 antibody, cells were first treated with antibody for 30 min, then 20 nM CXCL12 was added for three to four hours. The assay was followed the manufacturer's instruction, the LiveBLazer FRET-B/G Loading Kit (#K1030; Invitrogen) was added and the determine the fluorescence 520/477 nm by using fluorescence plate reader.

## Results

### *Expression of CXCR4 in cancer and normal cells*

To investigate the expression levels of CXCR4 in cancer, we conducted an analysis of mRNA levels derived from patients and corresponding standard samples, utilizing data from The Cancer Genome Atlas (TCGA) which provides RNA sequencing (RNA-seq) information. The expression profiles of CXCR4 in various tumor types compared to paired normal tissues are illustrated in **Figure 1A** and **1B**. Our findings indicate that the mRNA expression of CXCR4 is

significantly elevated in several cancer types compared to their normal tissue counterparts. Notably, we observed marked differences in CXCR4 levels between tumor and normal tissues in Breast Cancer (BRCA), Glioblastoma Multiforme (GBM), Kidney Renal Clear Cell Carcinoma (KIRC), Acute Myeloid Leukemia (LAML), Ovarian Cancer (OV), and Pancreatic Adenocarcinoma (PAAD), with statistical significance established at  $P < 0.05$ . These results underscore the critical role of CXCR4 in cancer pathogenesis

### *Prediction of CXCR4-CXCL12 binding region using AlphaFold3*

Since GPCRs are difficult to purify and crystallize due to their complex transmembrane structures. This complexity hinders the determination of their complete structures, which is crucial for drug design. Therefore, we utilized the protein structure prediction tool AF3 to generate an accuracy model of the CXCR4-CXCL12 complex, we have chosen high score model with ipTM and pTM scores of 0.78 and 0.79, respectively. This high-confidence model reveals key molecular interactions critical for ligand binding, as shown in (**Figure 2A** and **2B**). Among the three key extracellular loops (ECL1, ECL2, and ECL3), ECL2 was identified as the most significant for ligand binding based on major interacting residues (**Figure 2C**). Our structural analysis revealed several interface residues in CXCR4-S178, C186, I185, D187, and F189 that participate in salt bridge formation, hydrophobic interactions, and hydrogen bonding with CXCL12. Specifically, a salt bridge is formed between D187 of CXCR4 and K1 of CXCL12 and polar interaction is found between C186 of CXCR4 with K1 of CXCL12, while a hydrophobic core is established by F189 and I185 of CXCR4 interacting with P32 and Y7 of CXCL12. Additionally, two hydrogen bonds are observed, with D181 of CXCR4 interacting with N30 of CXCL12, and S178 of CXCR4 forming a bond with N33 of CXCL12. In addition, although ECL1 has one amino acid interaction with CXCL12 and ECL3 has two amino acid interactions, as shown in (**Figure 2D**, **2E**). Based on the results of the (**Figure 2C**) analysis, we consider that ECL2 is the major region for ligand specificity. Our study highlights ECL2 as the important CXCL12 recognition site, providing valuable insights for antibody selection targeting the CXCR4 receptor.

## Selection of GPCR targeting antibody via Alphafold3

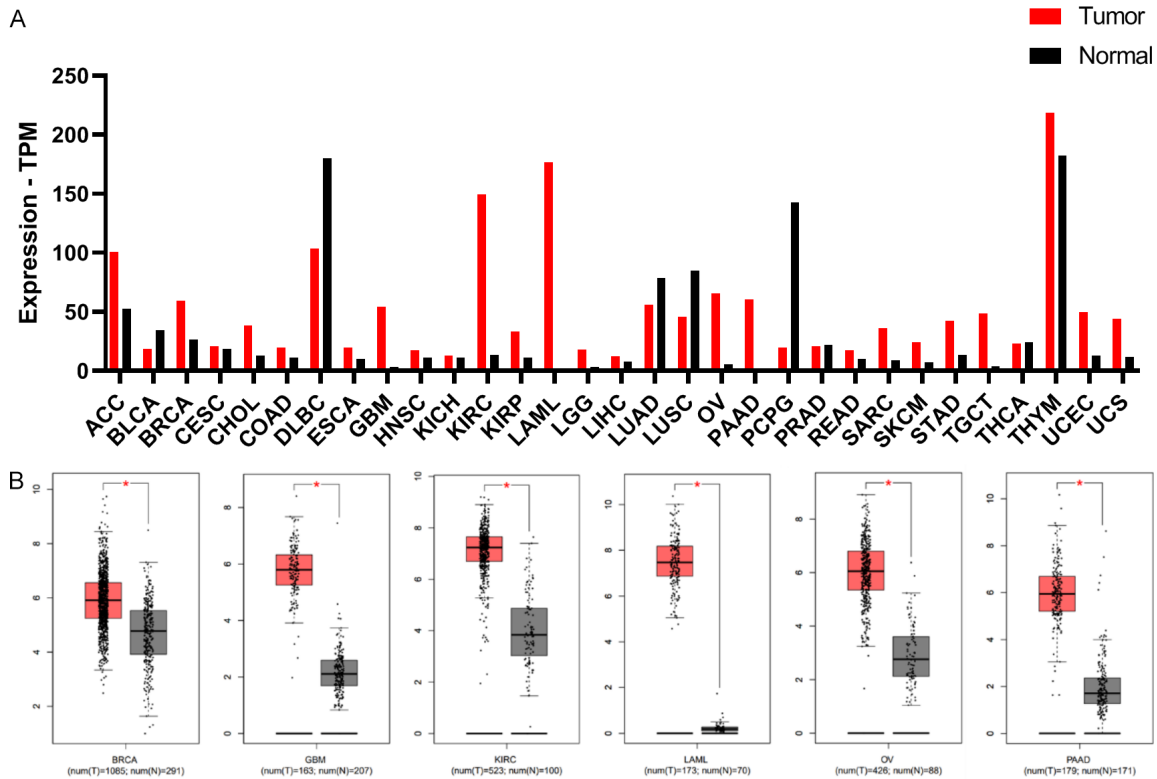


**Figure 1.** Comparison of CXCR4 between tumor samples and paired normal tissues. A. Expression of CXCR4 in tumor and normal tissues. Each dot represents expression of tumor type (red) or normal tissue (black). \* $P < 0.05$ . Kaplan-Meier plots of overall survival for patients with pancreatic cancer concerning the expression levels of SSEA-4 antigen. Abbreviations: ACC, adrenocortical carcinoma; BLCA, bladder urothelial carcinoma; BRCA, breast invasive carcinoma; CESC, cervical squamous cell carcinoma and endocervical adenocarcinoma; CHOL, cholangiocarcinoma; COAD, colon adenocarcinoma; DLBC, lymphoid neoplasm diffuse large B cell lymphoma; ESCA, esophageal carcinoma; GBM, glioblastoma multiforme; HNSC, head and neck squamous cell carcinoma; KICH, kidney chromophobe; KIRC, kidney renal clear cell carcinoma; KIRP, kidney renal papillary cell carcinoma; LAML, acute myeloid leukemia; LGG, brain lower grade glioma; LIHC, liver hepatocellular carcinoma; LUAD, lung adenocarcinoma; LUSC, lung squamous cell carcinoma; MESO, mesothelioma; OV, ovarian serous cystadenocarcinoma; PAAD, pancreatic adenocarcinoma; PCPG, pheochromocytoma and paraganglioma; PRAD, prostate adenocarcinoma; READ, rectum adenocarcinoma; SARC, sarcoma; SKCM, skin cutaneous melanoma; STAD, stomach adenocarcinoma; TGCT, testicular germ cell tumors; THCA, thyroid carcinoma; THYM, thymoma; UCEC, uterine corpus endometrial carcinoma; UCS, uterine carcinosarcoma. B. For BRCA, GBM, KIRC, LAML, OV, PAAD, normal tissues from the GTEx database were used as controls. \*,  $P < 0.05$ .

### Selection and characterization of isolated CXCR4-targeting antibodies

A schematic illustration of the CXCR4 receptor is shown in (Figure 3A), highlighting its key structural regions. The extracellular (EC) region includes the N-terminus and three extracellular loops (ECL), while seven transmembrane helices connect these loops. From AF3 result indicate that ECL2 of CXCR4 was shown for CXCL12 recognition, it presents a promising region for antibody selection against the CXCR4 receptor. To explore this, we synthesized the biotinylated ECL2 peptides and utilized it as a target in four-round biopanning process using a single-chain

variable fragment (scFv) combinatorial antibody library containing approximately  $10^{11}$  members. Following the panning process, multiple phage clones were identified, and sequencing analysis revealed several scFv candidates that exhibited high enrichment across the rounds. These enriched scFv sequences were subsequently sub-cloned into a pFuse expression vector for mammalian expression (Figure 3B). The purified recombinant antibodies were then subjected to enzyme-linked immunosorbent assay (ELISA) screening to assess their binding affinity against the ECL2 peptide as well as other CXCR4-related peptides, N-terminus peptide and ECL1-3. The

## Selection of GPCR targeting antibody via AlphaFold3

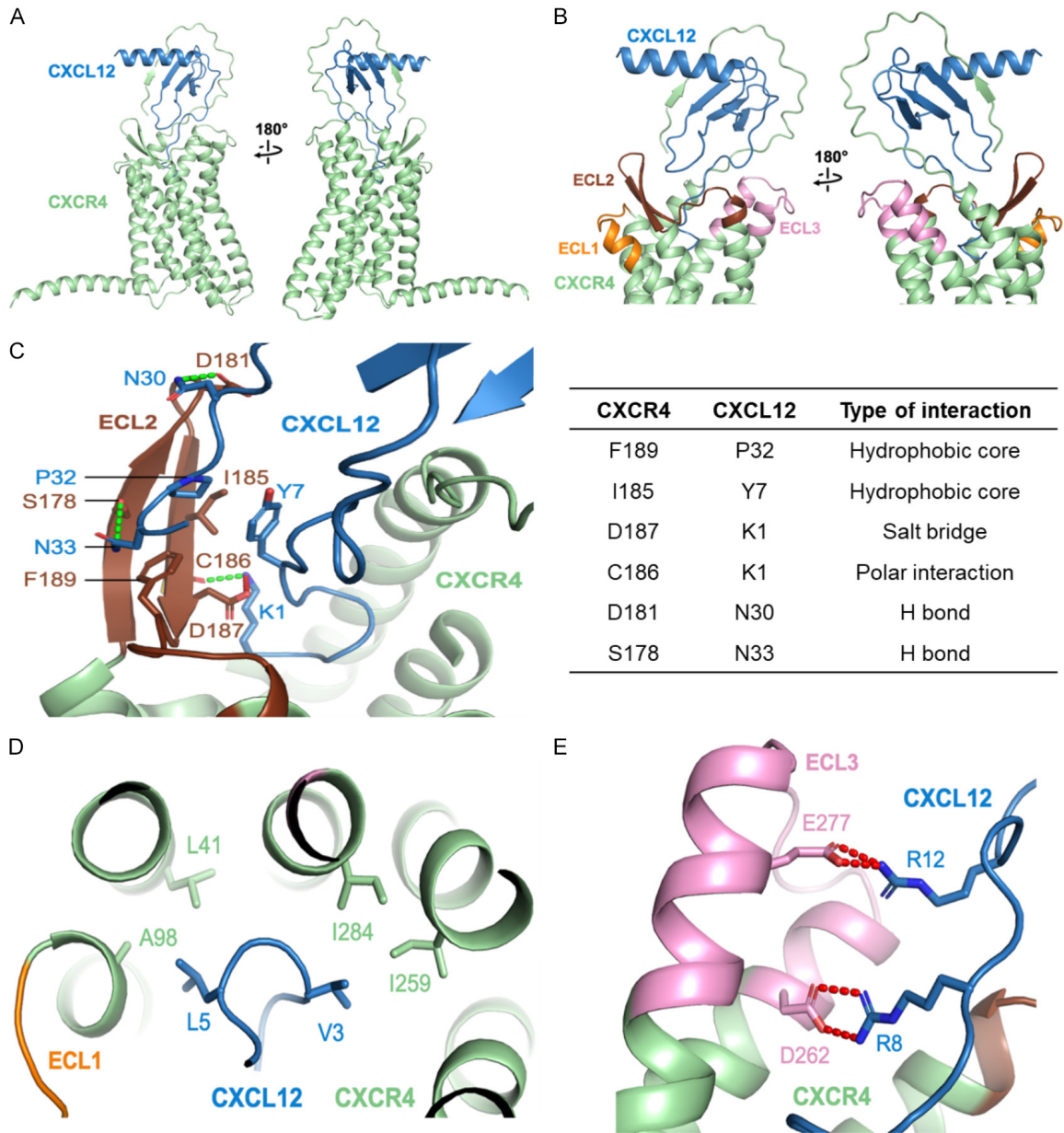


**Figure 2.** Predicted structure and interactions between CXCR4 and CXCL12 using AlphaFold3. **A.** The overall structure of the CXCR4-CXCL12 complex. **B.** A close-up view of the complex, with ECL1, ECL2 and ECL3 colored orange, brown and pink, respectively. **C.** ECL2 interactions with CXCL12, ECL2 and CXCL12 are represented in cartoon in maroon and blue color. Detailed residues interactions observed in the model. **D.** ECL1 interactions with CXCL-12, ECL1 and CXCL12 are represented in cartoon in orange and blue color respectively. **E.** ECL3 interactions with CXCL-12, ECL3 and CXCL-12 are represented in cartoon in pink and blue color. Hydrogen bonds are represented in red lines.

result (**Figure 3C**) showed the six scFv antibodies was confirmed their specificity for the ECL2 of CXCR4. Further characterization of the selected antibodies was performed using fluorescence-activated cell sorting (FACS) to determine their ability to recognize membrane-bound CXCR4 in a cellular context. The result (**Figure 3D**) show that five scFv antibodies dem-

onstrated binding to CXCR4-overexpressed 293T cells, confirming their specificity for the CXCR4. These results indicate the successful isolation of antibody clones that selectively recognize the ECL2 region of CXCR4, providing potential candidates for further characterization into their potential to inhibit CXCL12-CXCR4 interactions.

## Selection of GPCR targeting antibody via Alphafold3

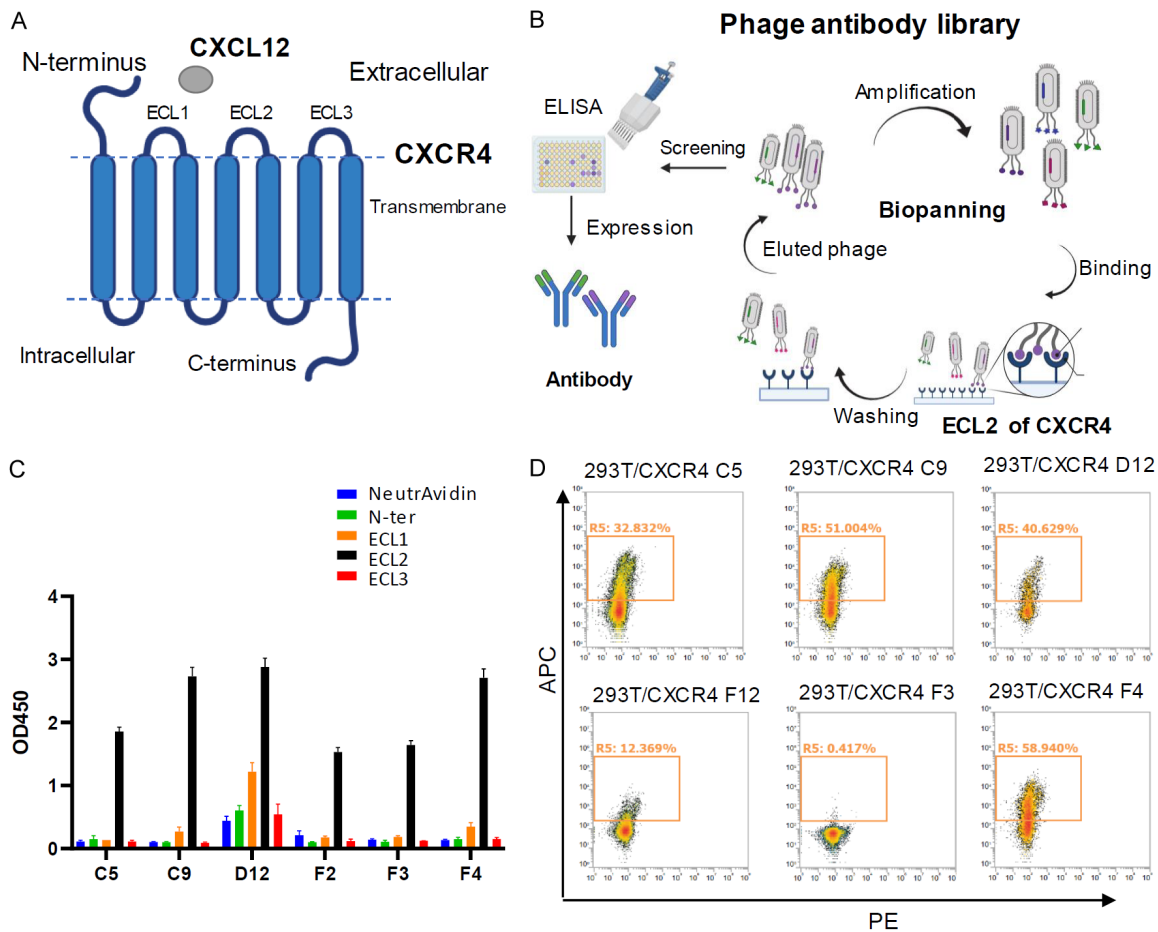


**Figure 3.** Selection and characterization of CXCR4-targeting antibodies from a phage display antibody library. A. Schematic representation of the CXCR4 receptor, highlighting the extracellular and intracellular regions. The EC region comprises the N-terminus and three extracellular loops (ECL1-ECL3). The seven transmembrane helices connecting these loops are also depicted. B. Strategy for the selection of CXCR4-targeting antibodies using an epitope-directed biopanning approach. The ECL2 region of CXCR4 was used as the primary epitope for four rounds of biopanning against a phage-displayed antibody library. Following selection, ELISA screening was performed to identify antibodies with specificity for ECL2. C. Validation of ECL2-specific antibody binding using biotinylated synthetic peptides corresponding to the N-terminal region (N-ter), ECL1, ECL2, and ECL3 of CXCR4. Binding specificity was confirmed by ELISA, demonstrating preferential recognition of ECL2 over other extracellular regions. D. Flow cytometric analysis of selected antibodies to assess binding to CXCR4 in 293T cells overexpressing CXCR4.

### *Evaluation of CXCL12-induced CXCR4 signaling inhibition by isolated CXCR4-targeting antibodies*

To determine whether isolated CXCR4-targeting antibodies inhibit CXCL12 binding and subsequent CXCR4-mediated signaling, we utilized Tango CXCR4- $\beta$ -lactamase (bla) U2OS reporter cells for evaluation. These reporter cells stably express human CXCR4 associated with a TEV protease site and a Gal4-VP16 transcription factor. Additionally, a bla reporter gene regulated by a UAS response element and a  $\beta$ -arrestin/TEV protease fusion protein are expressed by

the parental line. This reporter cell system allows for real-time monitoring of CXCR4 activation upon ligand stimulation. In the assay, CXCR4 reporter cells were treated with the natural ligand CXCL12 in the presence or absence of the isolated CXCR4 antibodies to evaluate their agonistic or antagonistic effects. The C5 antibody exhibited strong inhibitory activity against CXCL12-induced  $\beta$ -arrestin recruitment, effectively blocking downstream CXCR4 signaling. The F4 antibody also demonstrated partial inhibition of the signaling pathway. These results as shown in (Figure 4) suggest that C5 and F4 antibodies can modulate CXCR4

## Selection of GPCR targeting antibody via Alphafold3

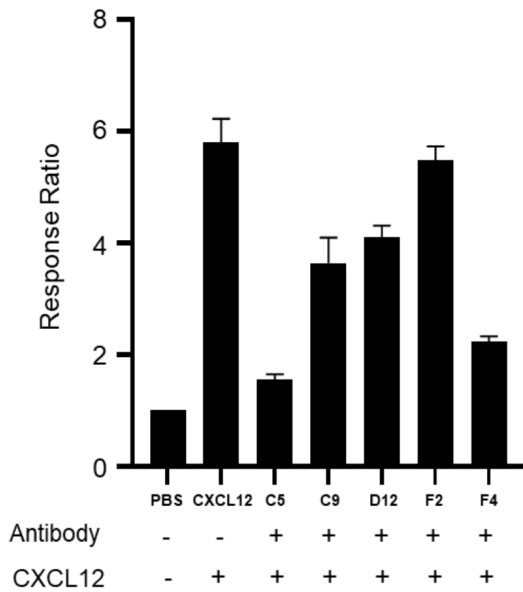


**Figure 4.** Evaluation of CXCL12-induced CXCR4 signaling inhibition by isolated CXCR4-targeting antibodies. Tango CXCR4-bla U2OS reporter cell line was used for evaluation of CXCL12-induced CXCR4 signaling. CXCL12 and isolated CXCR-4 antibodies were mixed with the reporter cells at 37 °C to measure their agonist effects following the manufacturer's instruction.

signaling by preventing natural ligand-induced activation, highlighting their potential for therapeutic applications targeting CXCR4-driven pathways.

### *CXCR4-targeting antibody induces antibody-dependent cell-mediated cytotoxicity in cancer cell lines*

To evaluate the ability of isolated CXCR4-targeting antibodies to induce immune-mediated cytotoxicity, we performed antibody-dependent cell-mediated cytotoxicity (ADCC) assays using acute T cell leukemia cell line and B lymphoma cell line. The cytotoxic activity of the antibodies was assessed in the presence of peripheral blood mononuclear cells (PBMCs), which provided natural killer (NK) cells and monocytes as effector cells. An effector-to-target (E:T) ratio of 10:1 was used, and cell death was quantified by measuring lactate dehydrogenase (LDH) release. As shown in (Figure 5), the C5 and F4 antibody mediated ADCC in T cell leukemia cell line Jurkat, B lymphoma cell line Romas when co-cultured with donor PBMCs. These results demonstrate that the C5, F4 antibody can trigger immune-mediated killing

of CXCR4-expressing cancer cells, highlighting its potential therapeutic application in targeting hematological malignancies.

### *Superimposed structure of experimental structure and Alphafold3 structure*

We performed a structural comparison by superimposing the experimentally determined Cryo electron microscopy (cryo-EM) structure of the CXCR4/CXCL12 complex (PDB ID: 8k3z) and the computationally predicted model using AF3. This superimposition was carried out to assess the protein topology and validate the accuracy of the AF3 model. The cryo-EM structure is depicted in yellow and orange, while the AF3-predicted model is shown in blue and green. The results, as illustrated in (Figure 6A), demonstrate that the predicted model closely aligns with the experimental cryo-EM complex structure. The structural alignment analysis reveals a root mean square deviation RMSD of 1.5 Å, and  $\alpha$  RMSD value of 1.3 Å, indicated a high degree of structural similarity between the two models. Additionally, we performed an analysis to superimpose specific binding interface of CXCR4 (ECL2) region, the result (Figure 6B) show that RMSD value of 0.5 Å and  $\alpha$  RMSD of 0.3 Å, demonstrating high structural consistency on the specific interface. We also superimposed interacting residues of cryo-EM structure regions with AF3 structure, the results (Figure 6C) showed that the primary interactions between CXCR4 and CXCL12 observed in the cryo-EM structure closely align with those predicted by AF3. This consistency highlights the reliability of the AF3-generated model in accurately predicting the overall structure of CXCR4 and its interaction with CXCL12. Furthermore, these findings support the use of AF3 as a powerful tool for structural modeling, facilitating the identification of key interaction sites for antibody screening and therapeutic development.

## Discussion

GPCRs are integral to various physiological processes as they facilitate signal transduction following the binding of specific ligands. This interaction initiates a cascade of cellular responses, highlighting the importance of GPCRs in maintaining homeostasis and mediating physiological functions. The extracellular regions, includ-

## Selection of GPCR targeting antibody via Alphafold3

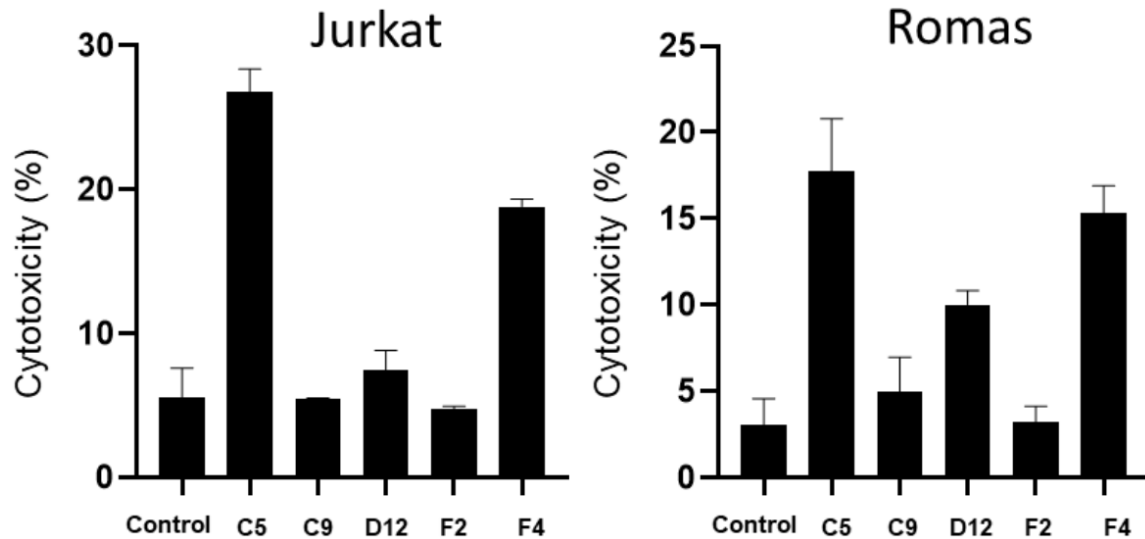


**Figure 5.** Cytotoxicity of isolated CXCR4 antibodies in cancer cell lines. The cancer cells (10,000 per well) and human peripheral blood mononuclear cells (hPBMCs) (100,000 per well) were incubated with different treatments in 96-well plates at 37 °C. After incubation, LDH release was quantified from 50  $\mu$ L of media supernatant. Specific killing was calculated by background subtraction and total lysis comparison according to the manufacturer's protocol.

ing the N-terminus and extracellular loops, enable the recognition of diverse ligands, leading to receptor activation. In many physiological and pathological conditions, ligand binding induces signaling pathway activation, a phenomenon known as biased agonism. This concept has been extensively studied, particularly in chemokine receptors. Despite their critical roles in physiological processes, dysregulation of GPCR signaling has been implicated in numerous pathological conditions, including autoimmune and inflammatory diseases, as well as cancers. Although GPCR are the largest drug-targeted, only about 80 GPCRs have been drugged with small molecules and mainly with peptides associated with natural endogenous ligands. The development of effective and specific therapeutic agents for these important targets persists as a significant challenge for the pharmaceutical industry. GPCRs are difficult to purify and crystallize due to their complex transmembrane structures. However, the structural characterization of GPCR-ligand interactions remains challenging due to difficulties in obtaining high-resolution co-crystal structures. Recent advances in AI, particularly AF3, have significantly improved protein structure prediction, offering new insights into molecular interactions. AF3 represents a major breakthrough in structural biology by enabling accurate modeling of complex biomolecular interactions,

including ligand-receptor binding. This capability is crucial for drug discovery, also help for understanding how ligands interact with GPCRs, which can lead to more effective and selective therapeutics.

In this study, we showed higher expression levels of CXCR4 and CXCL12 across different cancer types, suggesting their potential implications in cancer therapy. Structural characterization of GPCR-ligand interactions remains challenging due to the difficulty in obtaining complex structures. To address this, we first utilized AF3 to generate a complex model and then predicted the accuracy of the GPCR-ligand binding site. Subsequently, we compared the AF3 predictions with the recently reported cryo-EM structure of the CXCR4-CXCL12 complex described by Liu et al [36]. Their study revealed that CXCL12 is a flexible ligand capable of adopting different binding conformations when interacting with CXCR4. Using the cryo-EM structure as a reference, we validated our AF3 predictions and observed minor differences between the two models. Despite these minor differences in RMSD, the primary interacting residues in both structures remain unchanged, indicating that AF3 significantly predicts critical binding sites. The subtle variations observed do not affect the overall integrity of the complex and show key structural features and molecular

## Selection of GPCR targeting antibody via AlphaFold3

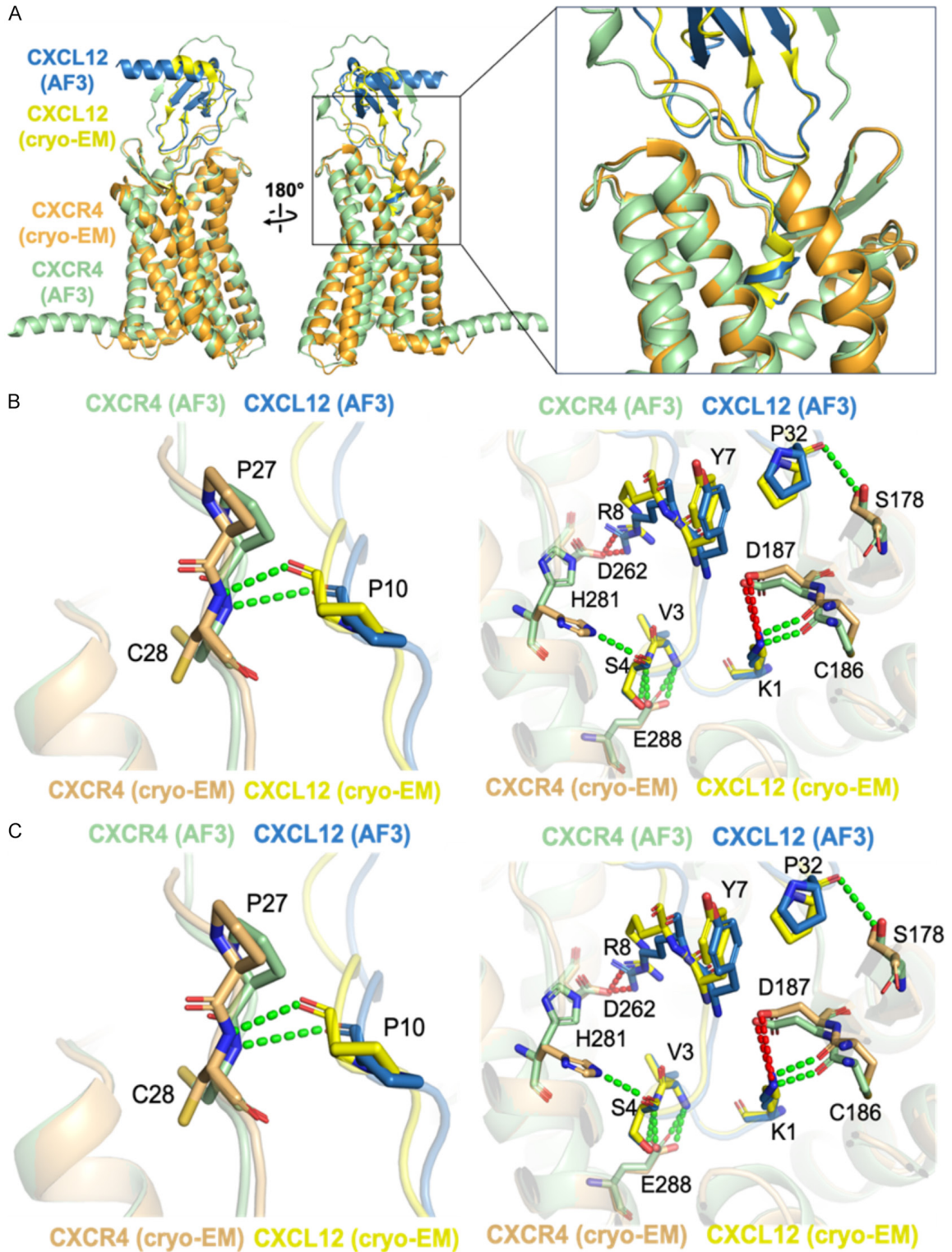


**Figure 6.** Superposition of Cryo-EM and AlphaFold 3 models of the CXCR4/CXCL12 complex. A. The Cryo-EM structure of the CXCR4/CXCL12 complex (PDB ID: 8K3Z) is shown in yellow and orange, while the AF3-predicted model is shown in blue and green. Structural comparison reveals a root mean square deviation (RMSD) of 1.5 Å, and ( $C\alpha$  RMSD) of 1.2 Å confirming the high accuracy of the AF3 model in replicating the overall architecture of CXCR4 and its interaction with CXCL12. B. Superposition of specific interface of CXCR-4 (ECL2) region with experimental structure, both are represented in sticks, showing higher structural similarity with the (RMSD) yield of 0.5 Å and ( $C\alpha$  RMSD) of 0.3 Å. AF3 region is represented in cyan and Cryo-EM structure is represented in orange. C. Super-

## Selection of GPCR targeting antibody via Alphafold3

position of the cryo-EM interacting complex interface with AF3 interacting complex interface, cryo-EM residues are represented in orange and yellow while AF3 interacting residues are represented in blue and green. The overall data represent that most of the primary interactions in cryo-EM structure aligns with alpha fold predicted model without changing integrity of the overall complex.

recognition patterns within the CXCR4-CXCL12 complex. These findings led us to focus on the ECL2 region for antibody selection, as it plays a crucial role in ligand recognition. Targeting ECL2 could provide a novel strategy for modulating CXCR4 signaling, offering potential therapeutic applications for diseases driven by this pathway. The alignment revealed that key interactions observed in the cryo-EM structure closely match those predicted by AF3, confirming its reliability for structural modeling.

In summary, understanding ligand-receptor interactions in GPCRs is fundamental for deciphering complex signaling networks and receptor dynamics. However, the structural characterization of GPCR-ligand interactions remains challenging due to difficulties in obtaining high-resolution co-crystal structures. Our approach, combining epitope-guided antibody selection with AF3 predictions, provides an efficient strategy to overcome these limitations. Importantly, this methodology can be extended to other GPCRs and cellular contexts, offering a versatile platform for developing therapeutic antibodies. Given the pivotal role of GPCRs and their ligands as therapeutic targets in various diseases, our results suggest promise for generating effective antibodies to treat CXCR4-expressing cancers and other GPCR-related disorders.

### Acknowledgements

This work was supported by China Medical University Yingcai Scholar Fund CMU110-YTY-03, National Science and Technology Council Taiwan (NSTC 113-2639-B-039-001-ASP and T-Star Center NSTC 113-2634-F-039-001), Ministry of Health and Welfare Taiwan (MOHW114-TDU-B-222-144016), and The Featured Areas Research Center Program by the Ministry of Education (MOE) in Taiwan.

### Disclosure of conflict of interest

None.

**Address correspondence to:** Kyung Ho Han, Department of Biological Sciences and Biotechnology,

Hannam University, Daejeon 34054, Republic of Korea. E-mail: kyungho1@hnu.kr; Chih-Wei Lin, Institute of Biochemistry and Molecular Biology, China Medical University, Taichung 406040, Taiwan. E-mail: cwlin25@mail.cmu.edu.tw

### References

- [1] Wang J, Hua T and Liu ZJ. Structural features of activated GPCR signaling complexes. *Curr Opin Struct Biol* 2020; 63: 82-89.
- [2] Masuho I, Kise R, Gainza P, Von Moo E, Li X, Tany R, Wakasugi-Masuho H, Correia BE and Martemyanov KA. Rules and mechanisms governing G protein coupling selectivity of GPCRs. *Cell Rep* 2023; 42: 113173.
- [3] Chaudhary PK and Kim S. An insight into GPCR and G-proteins as cancer drivers. *Cells* 2021; 10: 3288.
- [4] Kircher M, Herhaus P, Schottelius M, Buck AK, Werner RA, Wester HJ, Keller U and Lapa C. CXCR4-directed theranostics in oncology and inflammation. *Ann Nucl Med* 2018; 32: 503-511.
- [5] Rosenbaum DM, Rasmussen SG and Kobilka BK. The structure and function of G-protein-coupled receptors. *Nature* 2009; 459: 356-363.
- [6] Hauser AS, Attwood MM, Rask-Andersen M, Schiöth HB and Gloriam DE. Trends in GPCR drug discovery: new agents, targets and indications. *Nat Rev Drug Discov* 2017; 16: 829-842.
- [7] Congreve M, de Graaf C, Swain NA and Tate CG. Impact of GPCR structures on drug discovery. *Cell* 2020; 181: 81-91.
- [8] Zhang M, Chen T, Lu X, Lan X, Chen Z and Lu S. G protein-coupled receptors (GPCRs): advances in structures, mechanisms and drug discovery. *Signal Transduct Target Ther* 2024; 9: 88.
- [9] Thompson MD, Reiner-Link D, Berghella A, Rana BK, Rovati GE, Capra V, Gorvin CM and Hauser AS. G protein-coupled receptor (GPCR) pharmacogenomics. *Crit Rev Clin Lab Sci* 2024; 8: 641-684.
- [10] Guo Q, He B, Zhong Y, Jiao H, Ren Y, Wang Q, Ge Q, Gao Y, Liu X, Du Y, Hu H and Tao Y. A method for structure determination of GPCRs in various states. *Nat Chem Biol* 2024; 20: 74-82.
- [11] Duan J, He XH, Li SJ and Xu HE. Cryo-electron microscopy for GPCR research and drug discovery in endocrinology and metabolism. *Nat Rev Endocrinol* 2024; 20: 349-365.

## Selection of GPCR targeting antibody via AlphaFold3

- [12] Abramson J, Adler J, Dunger J, Evans R, Green T, Pritzel A, Ronneberger O, Willmore L, Ballard AJ, Bambrick J, Bodenstein SW, Evans DA, Hung CC, O'Neill M, Reiman D, Tunyasuvunakool K, Wu Z, Žemgulytė A, Arvaniti E, Beattie C, Bertolli O, Bridgland A, Cherepanov A, Congreve M, Cowen-Rivers AI, Cowie A, Figurnov M, Fuchs FB, Gladman H, Jain R, Khan YA, Low CMR, Perlin K, Potapenko A, Savy P, Singh S, Stecula A, Thillaisundaram A, Tong C, Yakneen S, Zhong ED, Zielinski M, Židek A, Bapst V, Kohli P, Jaderberg M, Hassabis D and Jumper JM. Accurate structure prediction of biomolecular interactions with AlphaFold 3. *Nature* 2024; 8016: 493-500.
- [13] Krishna R, Wang J, Ahern W, Sturmfels P, Venkatesh P, Kalvet I, Lee GR, Morey-Burrows FS, Anishchenko I, Humphreys IR, McHugh R, Vafeados D, Li X, Sutherland GA, Hitchcock A, Hunter CN, Kang A, Brackenbrough E, Bera AK, Baek M, DiMaio F and Baker D. Generalized biomolecular modeling and design with RoseTTAFold All-Atom. *Science* 2024; 384: eadl2528.
- [14] Baek M, McHugh R, Anishchenko I, Jiang H, Baker D and DiMaio F. Accurate prediction of protein-nucleic acid complexes using RoseTTAFoldNA. *Nat Methods* 2024; 21: 117-121.
- [15] Wang J, Lisanza S, Juergens D, Tischer D, Watson JL, Castro KM, Ragotte R, Saragovi A, Milles LF, Baek M, Anishchenko I, Yang W, Hicks DR, Expòsit M, Schlichthaerle T, Chun JH, Dauparas J, Bennett N, Wicky BIM, Muenks A, DiMaio F, Correia B, Ovchinnikov S and Baker D. Scaffolding protein functional sites using deep learning. *Science* 2022; 377: 387-394.
- [16] Sumida KH, Núñez-Franco R, Kalvet I, Pellock SJ, Wicky BIM, Milles LF, Dauparas J, Wang J, Kipnis Y, Jameson N, Kang A, De La Cruz J, Sankaran B, Bera AK, Jiménez-Osés G and Baker D. Improving protein expression, stability, and function with ProteinMPNN. *J Am Chem Soc* 2024; 146: 2054-2061.
- [17] Mullard A. FDA approves 100th monoclonal antibody product. *Nat Rev Drug Discov* 2021; 20: 491-495.
- [18] Song CH, Jeong M, In H, Kim JH, Lin CW and Han KH. Trends in the development of antibody-drug conjugates for cancer therapy. *Antibodies (Basel)*, 2023; 12: 72.
- [19] Tsuchikama K, Anami Y, Ha SYY and Yamazaki CM. Exploring the next generation of antibody-drug conjugates. *Nat Rev Clin Oncol* 2024; 21: 203-223.
- [20] Hsieh YY, Su YL, Kuan FC, Chen SG, Chang CL, Shao YY, Tsai CW and Liang YH. Continuing anti-EGFR monoclonal antibody after secondary resection significantly prolongs overall survival for patients with metastatic colorectal cancer who were responsive to first-line anti-EGFR monoclonal antibody plus chemotherapy doublet. *Am J Cancer Res* 2024; 14: 5909-5920.
- [21] Chen L, Xu C, Ren W, Yu L and Tang T. Predicting immunotherapy-related adverse events in late-stage non-small cell lung cancer with KARS G12C mutation treated with PD-1 inhibitors through combined assessment of LCP1 and ADPGK expression levels. *Am J Cancer Res* 2024; 14: 4803-4816.
- [22] Lu RM, Hwang YC, Liu JJ, Lee CC, Tsai HZ, Li HJ and Wu HC. Development of therapeutic antibodies for the treatment of diseases. *J Biomed Sci* 2020; 27: 1.
- [23] Alfaleh MA, Alsaab HO, Mahmoud AB, Alkayyal AA, Jones ML, Mahler SM and Hashem AM. Phage display derived monoclonal antibodies: from bench to bedside. *Front Immunol* 2020; 11: 1986.
- [24] Lin CW and Lerner RA. Antibody libraries as tools to discover functional antibodies and receptor pleiotropism. *Int J Mol Sci* 2021; 22: 4123.
- [25] Lin CW and Han KH. Antibody libraries as platforms to exploring target and receptor pleiotropy. *Isr J Chem* 2023; 63: e202300050.
- [26] Lerner RA, Grover RK, Zhang H, Xie J, Han KH, Peng Y and Yea K. Antibodies from combinatorial libraries use functional receptor pleiotropism to regulate cell fates. *Q Rev Biophys* 2015; 48: 389-394.
- [27] Song CH, Lin CW and Han KH. Cell cycle-based antibody selection for suppressing cancer cell growth. *FASEB J* 2025; 39: e70402.
- [28] Bleul CC, Wu L, Hoxie JA, Springer TA and Mackay CR. The HIV coreceptors CXCR4 and CCR5 are differentially expressed and regulated on human T lymphocytes. *Proc Natl Acad Sci U S A* 1997; 94: 1925-1930.
- [29] Brelot A, Heveker N, Montes M and Alizon M. Identification of residues of CXCR4 critical for human immunodeficiency virus coreceptor and chemokine receptor activities. *J Biol Chem* 2000; 275: 23736-23744.
- [30] Chen G, Wang W, Meng S, Zhang L, Wang W, Jiang Z, Yu M, Cui Q and Li M. CXC chemokine CXCL12 and its receptor CXCR4 in tree shrews (*Tupaia belangeri*): structure, expression and function. *PLoS One* 2014; 9: e98231.
- [31] Cancilla D, Rettig MP and DiPersio JF. Targeting CXCR4 in AML and ALL. *Front Oncol* 2020; 10: 1672.
- [32] Mezzapelle R, Leo M, Caprioglio F, Colley LS, Lamarca A, Sabatino L, Colantuoni V, Crippa MP and Bianchi ME. CXCR4/CXCL12 activities in the tumor microenvironment and implica-

## Selection of GPCR targeting antibody via AlphaFold3

- tions for tumor immunotherapy. *Cancers (Basel)* 2022; 14: 2314.
- [33] Scala S. Molecular pathways: targeting the CXCR4-CXCL12 axis-untapped potential in the tumor microenvironment. *Clin Cancer Res* 2015; 21: 4278-4285.
- [34] Mezzapelle R, De Marchis F, Passera C, Leo M, Brambilla F, Colombo F, Casalgrandi M, Preti A, Zambrano S, Castellani P, Ertassi R, Silingardi M, Caprioglio F, Basso V, Boldorini R, Carretta A, Sanvito F, Rena O, Rubartelli A, Sabatino L, Mondino A, Crippa MP, Colantuoni V and Bianchi ME. CXCR4 engagement triggers CD47 internalization and antitumor immunization in a mouse model of mesothelioma. *EMBO Mol Med* 2021; 13: e12344.
- [35] Shi X, Wan Y, Wang N, Xiang J, Wang T, Yang X, Wang J, Dong X, Dong L, Yan L, Li Y, Liu L, Hou S, Zhong Z, Wilson IA, Yang B, Yang G and Lerner RA. Selection of a picomolar antibody that targets CXCR2-mediated neutrophil activation and alleviates EAE symptoms. *Nat Commun* 2021; 12: 2547.
- [36] Liu Y, Liu A, Li X, Liao Q, Zhang W, Zhu L and Ye RD. Cryo-EM structure of monomeric CXCL12-bound CXCR4 in the active state. *Cell Rep* 2024; 43: 114578.